CLINICAL AND DIAGNOSTIC LABORATORY IMMUNOLOGY, Nov. 2000, p. 953–959 Vol. 7, No. 6
1071-412X/00/$04.00+0

T-Cell Receptor Vβ Repertoire CDR3 Length Diversity Differs within CD45RA and CD45RO T-Cell Subsets in Healthy and Human Immunodeficiency Virus-Infected Children

ZHONG CHEN KOU, JOSHUA S. PUHR, MABEL ROJAS, WAYNE T. McCORMACK, MAUREEN M. GOODENOW, AND JOHN W. SLEASMAN*

Department of Pediatrics, Division of Immunology and Infectious Diseases, and Department of Pathology, Immunology, and Laboratory Medicine, University of Florida College of Medicine, Gainesville, Florida

Received 3 May 2000/Returned for modification 11 July 2000/Accepted 3 August 2000

The T-cell receptor (TCR) CDR3 length heterogeneity is formed during recombination of individual Vβ gene families. We hypothesized that CDR3 length diversity could be used to assess the fundamental differences within the TCR repertoire of CD45RA and CD45RO T-cell subpopulations. By using PCR-based spectratyping, nested primers for all 24 human Vβ families were developed to amplify CDR3 lengths in immunomagnetically selected CD45RA and CD45RO subsets within both $CD4^+$ and $CD8^+$ T-cell populations. Umbilical cord blood mononuclear cells or peripheral blood mononuclear cells obtained from healthy newborns, infants, and children, as well as human immunodeficiency virus (HIV)-infected children, were analyzed. All T-cell subsets from newborn and healthy children demonstrated a Gaussian distribution of CDR3 lengths in separated T-cell subsets. In contrast, HIV-infected children had a high proportion of predominant CDR3 lengths within both CD45RA and CD45RO T-cell subpopulations, most commonly in $CD8^+$ CD45RO T cells. Sharp differences in clonal dominance and size distributions were observed when cells were separated into CD45RA or CD45RO subpopulations. These differences were not apparent in unfractionated $CD4^+$ or $CD8^+$ T cells from HIV-infected subjects. Sequence analysis of predominant CDR3 lengths revealed oligoclonal expansion within individual Vβ families. Analysis of the CDR3 length diversity within CD45RA and CD45RO T cells provides a more accurate measure of disturbances in the TCR repertoire than analysis of unfractionated CD4 and CD8 T cells.

During T-cell development the T-cell receptor (TCR) β chain is formed by the recombination of germ line-encoded variable (V)-, diversity (D)-, and joining (J)-region gene elements (23, 31). The hypervariable region of each TCR Vβ family, or the complementarity-determining region (CDR3), is formed by the joining of V-(D)-J segments, thereby establishing the diversity of the cellular immune response (14, 16, 24). Additional diversity is generated within CDR3 through the removal or insertion of non-germ-line nucleotides at each joining junction (16, 24). Therefore, the TCR CDR3 region varies in both length and amino acid sequence. This variability can discriminate between functionally distinct TCR clonotypes. Changes in CDR3 length and amino acid sequences can be used to monitor the course of the T-cell response to an antigen (12).

Human $CD4^+$ T cells can be subdivided into subsets of naive or memory T cells on the basis of the expression of either the high- or low-molecular-weight isoforms of the leukocyte common antigen, CD45RA or CD45RO, respectively (8). The majority of T cells in infants are derived from the thymus and express CD45RA (11), in contrast to adults, in whom the majority of T cells express the CD45RO T-cell phenotype (29). There is a postthymic differentiation pathway in which T cells lose the ability to express CD45RA and gain the ability to express CD45RO after an encounter with antigen (1, 8, 9). We hypothesized that the distribution of CDR3 lengths within any particular Vβ family would reflect this fundamental difference between CD45RA and CD45RO T cells. Using spectratyping, we developed a highly accurate and sensitive assay to measure differences in the distribution of CDR3 lengths in highly purified CD45RA and CD45RO T cells from healthy and human immunodeficiency virus (HIV)-infected children. Umbilical cord blood mononuclear cells provided a model for new thymic T-cell emigrants with a polyclonal TCR diversity (19). HIV-infected subjects served as a model to assess clonal dominance within T-cell subpopulations because of the marked skewing of the CDR3 length within $CD4^+$ and $CD8^+$ T cells from these individuals (10, 17, 30, 32). Spectratyping in combination with cell separation techniques that fractionate CD45RA and CD45RO T-cell subsets distinguish the extent of TCR diversity within individual Vβ families more accurately and with greater sensitivity than analysis of unfractionated T cells. Sequence analysis of CDR3 length diversity in CD45RA and CD45RO T-cell subpopulations can be used to define the extent of clonal expansion within the TCR repertoire.

MATERIALS AND METHODS

Subjects. The study consisted of a cross-sectional analysis of umbilical cord or peripheral blood samples obtained from three healthy newborns, two infants, and two children. Additional samples were obtained from four HIV-infected children at different Centers for Disease Control and Prevention (CDC) clinical and immune stages of HIV disease prior to the initiation of antiretroviral therapy. Blood samples were obtained by a protocol approved by the Institutional Review Board of the University of Florida.

Isolation and purification of T-lymphocyte subsets. Umbilical cord blood mononuclear cells and peripheral blood mononuclear cells (PBMCs) were isolated by Ficoll-Hypaque centrifugation. Separation of T-cell subpopulations from umbilical cord blood and PBMCs was carried out by previously described methods (2, 28). $CD4^+$ T lymphocytes were selected by using magnetic multisort microbeads coated with an anti-CD4 monoclonal antibody (Miltenyi Biotech, Auburn, Calif.) and a magnetic cell-sorting (MACS) high-gradient magnetic separation column. Microbeads coated with monoclonal antibody and mononuclear cells were mixed and incubated at 4°C for 15 min. Labeled $CD4^+$ cells

* Corresponding author. Mailing address: Department of Pediatrics, Division of Immunology and Infectious Diseases, College of Medicine, University of Florida, Box 100296, 1600 S.W. Archer Rd., Gainesville, FL 32610-0296. Phone: (352) 392-2961. Fax: (352) 392-0481. E-mail: Sleasjw@peds.ufl.edu.

TABLE 1. TCR Vβ and Cβ gene primers

First-round PCR primers		Nested PCR primers	
Primer	Sequence	Primer	Sequence
Vβ1	5′-GAT TCT GGA GTC ACA CAA ACC CCA AAG-3′	Vβ1NS	5′-GAA CTA AAC CTG AGC TCT C-3′
Vβ2	5′-GAG CTG GGT TAT CTG TAA GAG-3′	Vβ2NS	5′-GCT TCT ACA TCT GCA GTG C-3′
Vβ3	5′-GAT GTG AAA GTA ACC CAG AGC TCG AG-3′	Vβ3NS	5′-CTG GAG TCC GCC AGC ACC-3′
Vβ4	5′-CAA GTC GAT AGC CAA GTC ACC ATG-3′	Vβ4NS	5′-GAA GAC AGC AGC ATA TAT C-3′
Vβ5.1	5′-CCC TGG TCG ATT CTC AGG GCG CCA G-3′	Vβ5.1NS	5′-CTC GGC CCT TTA TCT TTG CG-3′
Vβ6	5′-CTG GAG TCT CCC AGA ACC CCA GAC AC-3′	Vβ6NS	5′-GAT CCA GCG CAC AGA GCA G-3′
Vβ7	5′-CAT GGG AAT GAC AAA TAA GAA GTC-3′	Vβ7NS	5′-GAA TGC CCC AAC AGC TCT C-3′
Vβ8	5′-CGT TCC GAT AGA TGA TTC AGG GAT GC-3′	Vβ8NS	5′-GCC CTC AGA ACC CAG GGA C-3′
Vβ9	5′-GAA ACG ACA AGT CCA TTA AAT G-3′	Vβ9NS	5′-CCC TGG AGC TTG GTG ACT CTG-3′
Vβ10	5′-GAC ACC AAG GTC ACC CAG AGA CC-3′	Vβ10NS	5′-GGA GAT CCA GTC CAC GGA G-3′
Vβ11	5′-GAA GCT GAC ATC TAC CAG ACC CCA AG-3′	Vβ11NS	5′-GGA GTC TGC CAG GCC CTC-3′
Vβ12	5′-CTG ACA AAG GAG AAG TCT CAG-3′	Vβ12NS	5′-CTC TGG AGT CGC TAC CAG-3′
Vβ13	5′-GAC CCA GGC ATG GGG CTG AAG CTG-3′	Vβ13NS	5′-GAT TTC CCG CTC AGG CTG G-3′
Vβ14	5′-GAT GTT CCT GAA GGG TAC AAA G-3′	Vβ14NS	5′-CGA AAA GAG AAG AGG AAT TTC-3′
Vβ15	5′-GTG TCT CTC GAC AGG CAC AGG C-3′	Vβ15NS	5′-CCC TAG AGT CTG CCA TCC-3′
Vβ16	5′-CTT AGC TGA AAG GAC TGG AGG GAC G-3′	Vβ16NS	5′-CTG CAG AAC TGG AGG ATT C-3′
Vβ17	5′-CTG AAG GGT ACA GCG TCT CTC GGG AG-3′	Vβ17NS	5′-CCA AAA GAA CCC GAC AGC TTT C-3′
Vβ18	5′-CAA ATG CCG GCG TCA TGC AGA ACC-3′	Vβ18NS	5′-GCG AGG AGA TTC GGC AGC-3′
Vβ19	5′-GCC AAA GTC ACA CAG ACT CCA GG-3′	Vβ19NS	5′-GCC CCA AGA ACG CAC CCT GC-3′
Vβ20	5′-GAA TCT CTC AGC CTC CAG AC-3′	Vβ20NS	5′-CCA GGA CCG GCA GTT CAT C-3′
Vβ21	5′-GCA GCC TGT GGC TTT TTG GTG C-3′	Vβ21NS	5′-CCA GCC TGC AGA GCT TGG-3′
Vβ22	5′-CAG ATG GGA CAG GAA GTG-3′	Vβ22NS	5′-CTC TGA AGA TCC GGT CCA C-3′
Vβ23	5′-GAT CGA TTC TCA GCT CAA CAG-3′	Vβ23NS	5′-CTC CTT GGA GCT GGG GGA C-3′
Vβ24	5′-GGC CGA ACA CTT CTT TCT GC-3′	Vβ24NS	5′-GAC ATC CGC TCA CCA GGC CTG-3′
Cβ	5′-CCC CAG GCC TCG GCG CTG ACG ATC TGG G-3′	CβNS[a]	5′-GTT TCT TCT GCT TCT GAT GGC TCA AAC ACA G-3′

[a] 6-FAM labeling.

which adhered to the column were washed three times with wash buffer and collected. $CD8^+$ T cells were selected after depletion of the $CD4^+$ cells by using microbeads coated with anti-CD8 monoclonal antibody (Miltenyi Biotech) and the MACS magnetic separation column. Purified $CD4^+$ or $CD8^+$ cells were released from the beads by using release reagent at 4°C for 15 min. The T-cell subpopulations were subsequently separated into $CD45RA^+$ or $CD45RO^+$ subpopulations by using the microbeads coated with the appropriate monoclonal antibodies (Miltenyi Biotech). The purity of each T-cell subpopulation was >90%, as determined by flow cytometry analysis.

Extraction of mRNA and synthesis of cDNA. Lymphocyte mRNA was isolated and purified by previously published techniques (6, 7). Briefly, mRNA was extracted from 1×10^5 to 5×10^5 purified T lymphocytes by using guanidinium isothiocyanate and a spin column with oligo(dT)-cellulose (mRNA purification kit; Pharmacia, Piscataway, N.J.). First-strand cDNA was synthesized by mixing mRNA with 1 μg of random hexanucleotides (Promega, Madison, Wis.) and 5 μl of supertranscriptase II (Gibco BRL, Grand Island, N.Y.) in a total volume of 20 μl at 37°C for 1 h. The reaction was terminated by heating at 70°C for 10 min.

PCR amplification of CDR3 cDNA. CDR3 size analysis within the TCR β chain was performed by a two-step PCR as described previously (5, 21). Separate amplification reactions for each of 24 human Vβ gene families were carried out in 25-μl reaction mixtures containing 0.5 μl (20 μM) each of the forward Vβ primer and the reverse Cβ primer, 0.5 μl (10 mM) of each deoxynucleoside triphosphate, 2.5 μl of 10× PCR buffer, 20.5 μl of sterile H_2O, 0.25 μl of cDNA, and 1.25 U of *Taq* polymerase. Amplifications were started with an initial denaturation step of 3 min at 95°C, followed by 35 cycles of 95°C for 1 min, 55°C for 1 min, and 72°C for 1 min, with a final extension step of 7 min. Primer sequences are shown in Table 1.

The second-round PCR used the first-round products as the template and a pair of nested PCR primers (Table 1); the forward primer (VβNS) was nested 3′ to the first-round Vβ-specific primer, and the reverse primer (CβNS) was located 88 bp away from the CDR3 region. The reverse primer (CβNS) contained a nontemplate sequence, GTTTCTT, on the 5′ end, which was labeled at the 5′ end with a blue fluorescent dye (6-FAM). To increase the amplification specificity, the primer concentrations were reduced to 5 μM in a 25-μl reaction mixture. Second-round amplification was performed at 94°C for 30 s, 55°C for 30 s, and 72°C for 30 s for 20 cycles.

Analysis of CDR3 length by spectratyping. Fluorescent PCR products and a size marker (ROX400; Perkin-Elmer Biosystems, Foster City, Calif.) were mixed with formamide and were denatured at 94°C for 2 mins. Samples were loaded onto a 6% acrylamide sequencing gel (National Diagnostic, Atlanta, Ga.) on a 24-lane Applied Biosystems model 373 DNA sequencer and were run for 6 h. The data were analyzed and quantified by using ABIPRISMGeneScan analysis software, which calculates the relative intensity of each product to generate a curve for each Vβ family.

Molecular cloning and sequencing of CDR3 segments. First-round PCR products were amplified with identical forward and reverse Vβ PCR primers but without the fluorescent label used for spectratyping of individual families. The second-round products were used for TA cloning and sequencing. The PCR products were purified by using a gel extraction kit (QIAGEN, Valencia, Calif.) according to the manufacturer's recommendation. They were directly cloned into TA cloning vector PCR 2.1 (Invitrogen Corporation, Carlsbad, Calif.), sequenced with fluorescent dideoxy terminators, and analyzed on an Applied Biosystems model 337A automated sequencer. The CDR3 amino acid sequence was analyzed by using DNAMAN software.

RESULTS

PCR-based spectratyping of CDR3 length diversity in T-cell lines, PBMCs, and umbilical cord mononuclear cells. Nested forward primers for each of the 24 human Vβ gene families were designed and used in combination with a nested (CβNS) reverse primer for PCR amplification of the TCR CDR3 region. The amplified CDR3 length was defined as the region between the upstream amino acid CASS residues in the Vβ segments and the downstream GXG box in the Jβ region (31). Jurkat cells, T cells that express TCR Vβ8 and that have a CDR3 length of 11 amino acids, were used as a control to optimize the spectratyping analysis (27). Amplification of Jurkat cDNA with Vβ8 and Cβ primers produced a single peak. Sequence analysis of the cloned Jurkat PCR products revealed that 10 of 10 clones had the identical sequence (CASSFSTC SANYGYTFGSG).

Amplification of cDNA from umbilical cord blood samples or PBMCs from healthy children resulted in CDR3 patterns that consisted of 7 to 10 different peaks for each Vβ family (Fig. 1A and B). Each peak in the CDR3 size patterns was spaced by three nucleotides (e.g., 1 amino acid). As shown in Fig. 1, all 24 Vβ families could be amplified with these primers. Repeated spectratyping analysis of the same cDNA samples revealed the identical patterns of the TCR Vβ CDR3 sizes (data not shown).

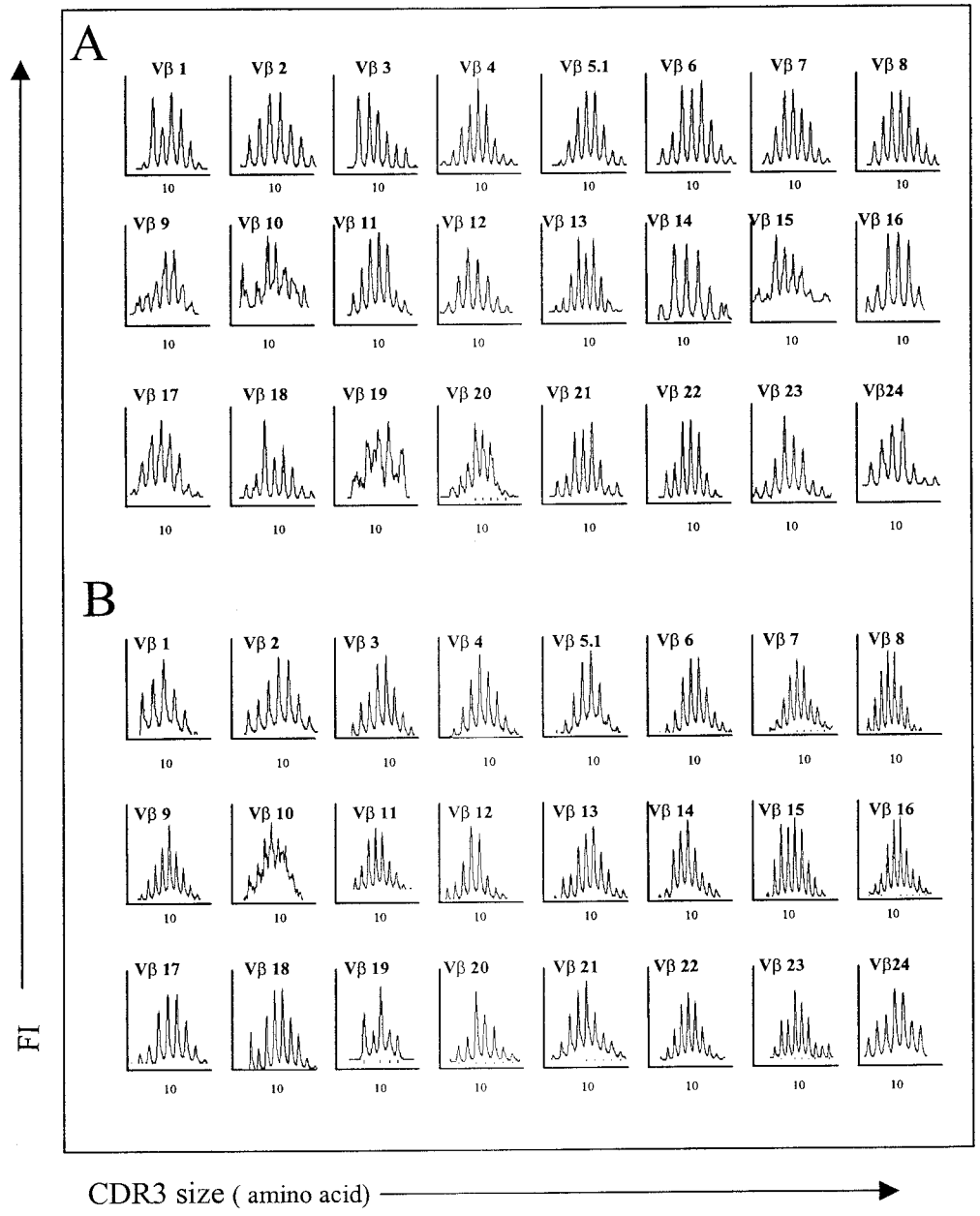

FIG. 1. Spectratyping of CDR3 sizes for all 24 Vβ gene families in healthy newborns and children. Two representative CDR3 size analyses for the 24 human Vβ gene families are shown for cDNAs obtained from umbilical cord T cells from a healthy newborn infant (A) and cDNAs obtained from T cells obtained from a healthy 12 year old (B). CDR3 size is shown on the *x* axis, and relative peak intensity (fluorescence intensity [FI]) is shown on the *y* axis. The peak size corresponding to CDR3 lengths of 10 amino acids are shown for each Vβ family.

Quantitation of amplified CDR3 lengths within individual Vβ families. The intensity of an individual peak reflects the relative representation of the particular CDR3 sizes within the individual Vβ family. The relative fluorescence intensity for individual CDR3 sizes can be quantified as the area under each peak (17). The data, when expressed as a percentage of the total area under the curves for each Vβ family, can be used to accurately determine the degree of CDR3 length diversity within any particular Vβ family. This analysis of length differences allows comparisons of TCR diversity among different Vβ families or among multiple individuals. A representative analysis of the size distribution of CDR3 lengths from $CD8^+$ CD45RO T cells obtained from a healthy child reveals a Gaussian-like distribution that ranges from 7 to 15 amino acids in length (Fig. 2A). Extremes in CDR3 lengths make up a minority (<1%) of the size diversity, while CDR3 sizes of 10, 11, and 12 amino acids make up 18, 24, and 23% of the area under the curve, respectively. In contrast, an HIV-infected subject, whose CDR3 size distribution demonstrates clonal dominance, has a predominant peak of eight amino acids in length, which encompasses over 80% of the area under the curve (Fig. 2A). All four HIV-infected children displayed perturbations within their $CD8^+$ CD45RO T-cell subpopulations. The number of Vß families exhibiting oligoclonal expansion were 50, 29, 58,

A

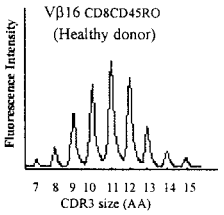

CDR3 size (AA)	7	8	9	10	11	12	13	14	15
Relative peak(%)	<1	3.5	9.3	18.0	24.0	23.0	12.5	5.5	1.5

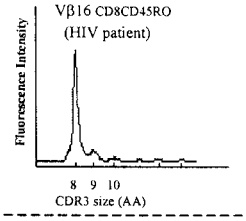

CDR3 size (AA)	7	**8**	9	10	11	12	13	14	15
Relative peak(%)	<1	**82**	11	3.5	<1	<1	<1	<1	<1

B

Clone	Vβ	N1 +Dβ +N2	Jβ	CDR3 length (Amino Acid)	Frequency
SJ8O1602	**CASS**	**VDRV**	**KAFFGQG**	**8**	**9/12 (75%)**
SJ8O1604	CASS	PDREG	LAFFGQG	9	1/12 (8%)
SJ8O1610	CASS	QRRIG	ELFFGPG	9	1/12 (8%)
SJ8O1612	CASS	GRLARD	EQFFGEG	10	1/12 (8%)

FIG. 2. Quantitation and sequence analysis of populations of CDR3 size fragments in healthy and HIV-infected individuals. (A) Relative distribution of CDR3 size distribution in $CD8^+$ CD45RO T cells from two representative subjects. The upper panel is CDR3 sizes in Vβ16 from a healthy child, and the lower panel is CDR3 sizes in Vβ16 from T cells from an HIV-infected child. The relative contribution of each CDR3 size (in amino acid [AA] length) is determined by the relationship of the peak to the total area under the curve. The results are shown as a percentage, as determined with ABIPRISM Gene Scan software. (B) Frequency of individual CDR3 clonotypes within $CD8^+$ CD45RO T cells from the HIV-infected subject whose results are shown in the lower panel of panel A. In a separate PCR amplification, the products for Vβ16 were cloned and 12 individual clones were sequenced. Nine of the 12 clones (75%) were 9 amino acids in length and had identical N1-Dβ-N2 and Jβ amino acid sequences. The other three clones had different lengths and amino acid sequences.

and 75% in the four children, respectively (data not shown). In contrast, in healthy children less than 5% of the Vß families from $CD8^+$ CD45RO T cells showed perturbations.

The degree of CDR3 size variability in umbilical cord mononuclear cells was determined to test the reproducibility of the analysis when applied to a group of healthy newborn subjects, who should have similar CDR3 size distributions and for whom there should be minimal variation between families or between subjects. The mean percentage and standard deviations for each CDR3 size among the three infants are summarized for seven representative Vβ families (Table 2). The CDR3 size distributions for all 24 Vβ families showed similar Gaussian distributions.

Sequence analysis of predominant CDR3 lengths. A predominant peak in any given CDR3 pattern may reflect oligoclonal expansion of T cells expressing a particular TCR or a polyclonal collection of T cells containing multiple TCRs of the same CDR3 size. We determined if predominant peaks were polyclonal or oligoclonal by directly sequencing the amplified CDR3 regions. The predominant CDR3 peak shown in Fig. 2A for the HIV-infected child had a length of 8 amino acids and accounted for 82% of Vβ16 CDR3 lengths. In separate PCRs second-round products were sequenced and compared to the sequences of products from a healthy subject whose CDR3 lengths demonstrated a Gaussian distribution. Twelve clones from the HIV-infected child were sequenced and four different amino acid sequences were identified. As shown in Fig. 2B, 9 of the 12 clones that were 8 amino acids in length had identical sequences. The sequences obtained from the healthy child showed no predominant clone (data not

TABLE 2. Mean percentage and standard deviations for each CDR3 size among three healthy infants in seven representative Vβ families

Vβ family	Mean (±SD) % relative intensity of CDR3 with the following no. of amino acids:								
	6	7	8	9	10	11	12	13	14
Vβ2	<1.0	3.3 (1.5)	10.4 (1.9)	18.5 (3.5)	25.0 (0.6)	22.0 (2.3)	11.6 (1.1)	5.9 (2.3)	2.0 (0.8)
Vβ5.1	<1.0	1.0 (0.2)	5.8 (2.1)	16.4 (2.9)	26.5 (0.5)	27.2 (1.4)	14.9 (1.8)	6.0 (1.6)	2.4 (0.6)
Vβ8	<1.0	4.3 (1.7)	9.7 (3.0)	19.4 (2.6)	23.9 (2.7)	22.9 (3.0)	12.2 (0.5)	5.7 (0.6)	2.0 (0.5)
Vβ12	<1.0	4.3 (0.7)	12.6 (3.6)	26.5 (5.2)	28.4 (4.0)	18.8 (7.0)	6.5 (1.3)	2.2 (0.6)	2.4 (0.6)
Vβ14	1.1 (0.3)	4.8 (2.8)	12.0 (9.0)	20.7 (5.0)	23.6 (3.6)	21.0 (7.5)	10.7 (5.4)	3.9 (2.7)	1.4 (1.8)
Vβ17	<1.0	1.9 (0.3)	8.0 (3.6)	19.3 (3.7)	23.9 (1.7)	26.5 (0.7)	13.3 (2.7)	5.0 (1.8)	1.9 (0.8)
Vβ22	<1.0	2.6 (0.2)	8.8 (1.2)	16.5 (5.6)	25.0 (0.9)	25.7 (1.2)	14.3 (6.0)	5.6 (2.3)	1.5 (0.3)

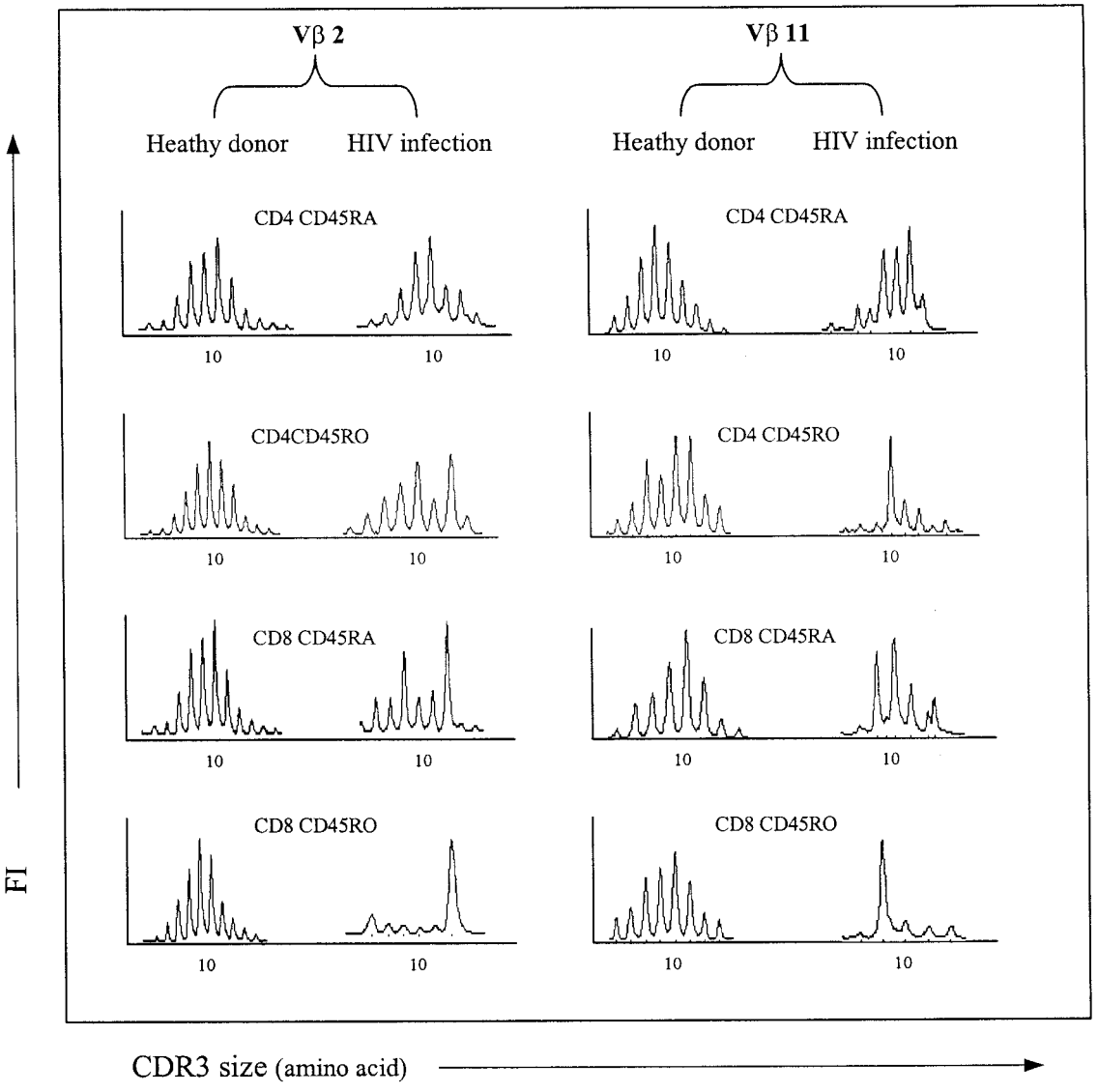

FIG. 3. Differences in CDR3 spectratyping of T-cell subpopulations for two Vβ families from healthy and HIV-infected children. T cells from a healthy 5-year-old subject and an age-matched HIV-infected subject whose HIV infection is CDC stage A1 were separated into $CD4^+$ CD45RA, $CD4^+$ CD45RO, $CD8^+$ CD45RA, and $CD8^+$ CD45RO T cells. CDR3 sizes are shown on the *x* axis, and fluorescence intensity (FI) is shown on the *y* axis. The CDR3 amino acid lengths corresponding to 10 amino acids are shown for each Vβ family.

shown). Sequence analysis confirms that the predominant CDR3 peaks represent an oligoclonal expansion of T cells.

Comparison of CDR3 size distribution on CD45RA and CD45RO T-cell subpopulations. The CDR3 length within the 24 Vβ gene families was determined by two-step PCR amplification of cDNA obtained from purified CD45RA or CD45RO from both $CD4^+$ and $CD8^+$ T cells isolated from PBMCs or umbilical cord blood samples from neonates, healthy children, and HIV-infected children. Neonatal cord blood samples demonstrated a Gaussian pattern similar to the results shown in Table 2 within $CD4^+$ CD45RA, $CD4^+$ CD45RO, $CD8^+$ CD45RA, and $CD8^+$ CD45RO in all families (data not shown). In contrast, there were differences in CDR3 size distributions when cDNAs from CD45RA and CD45RO T cells from healthy and HIV-infected subjects were compared (Fig. 3). For healthy children the lengths of CDR3 from both $CD4^+$ and $CD8^+$ T cells maintained a Gaussian distribution.

For all four asymptomatic HIV-infected children we observed predominant peaks within three or more Vβ families. In most cases expanded CDR3 lengths made up more than 50% of the total area under the curve for CDR3 sizes within the individual Vβ family. For the representative infected subject whose results are presented in Fig. 3, the Vβ2 CDR3 length containing 12 amino acids was the predominant peak within $CD8^+$ CD45RO T cells. Predominant peaks and perturbations away from the normal Gaussian distribution were also apparent within $CD4^+$ CD45RO T cells and $CD8^+$ CD45RO T cells for Vβ11 CDR3 lengths for this same subject. This degree of perturbation was undetectable in T-cell subpopulations from the age-matched healthy child.

Optimization of our ability to detect CDR3 size perturbations within individual Vβ families required further separation of $CD4^+$ and $CD8^+$ T cells into CD45RA and CD45RO subpopulations. As demonstrated in Fig. 4, clonal expansions within $CD4^+$ or $CD8^+$ T cells were not evident unless the cells were further fractionated. For the HIV-infected subject whose

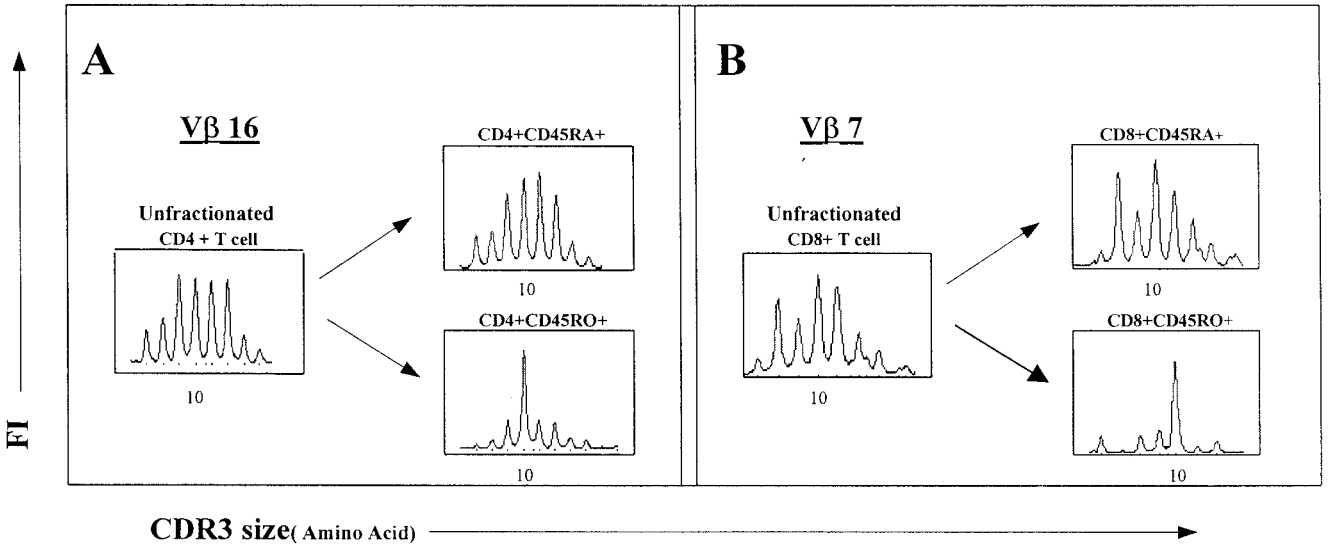

FIG. 4. Separation of $CD8^+$ T cells and $CD4^+$ T cells into CD45RA and CD45RO subpopulations distinguishes differences in CDR3 length distributions. $CD4^+$ and $CD8^+$ T cells from an HIV-infected child were further separated into CD45RA and CD45RO T cells, and the results were compared to the spectratyping analysis of CDR3 lengths from unseparated T cells. CDR3 sizes are shown on the *x* axis, and fluorescence intensity (FI) is shown on the *y* axis. The CDR3 amino acid lengths corresponding to 10 amino acids are shown for each Vβ family.

results are shown in Fig. 4, $CD4^+$ and $CD8^+$ T cells expressing Vβ16 and Vβ7, respectively, did not appear to contain perturbations unless they were fractionated into CD45RA and CD45RO subpopulations. Separation clearly shows the predominant peak within the CD45RO subsets of both the $CD4^+$ and $CD8^+$ T-cell populations.

DISCUSSION

Analysis of TCR CDR3 length by PCR-based spectratyping provides a powerful tool for the assessment of human TCR diversity in vivo and the evaluation of TCR diversity in health and disease states (4, 13, 18, 22, 25). In previous studies analysis of CDR3 size diversity has been focused on evaluations of unfractionated $CD4^+$ and $CD8^+$ T cells (6, 15, 17, 25, 30). In addition, the availability of primers for all 24 human Vβ families has been limited (13, 20). Many Vβ forward primers have failed to provide the degree of resolution needed to allow distinct definition and quantitation of individual CDR3 lengths. These limitations have led to the underutilization of TCR spectratyping in assessments of T-cell disorders. We have benefited from these earlier studies and have developed PCR primers and amplification conditions that result in accurate and reproducible CDR3 spectratyping of the 24 human Vβ families. Our modifications allow assessment of the relative diversity of CDR3 lengths within individual Vβ families and comparison of results between healthy and immune compromised individuals.

Our success in obtaining a high resolution between CDR3 peaks is due to the specificity of the Vβ forward primers and the placement of the seven nontemplate nucleotides on the 5′ ends of the reverse primers (3′-CβNS). These additional nucleotides ensure the catalytic addition of nontemplate nucleotides to the 3′ ends of the amplified products by *Taq* DNA polymerase. The 7-bp nucleotides also result in a high level of adenylation of the 3′ end of the forward DNA strand to facilitate accurate spectratyping and TA cloning (3). We were able to confirm both the accuracy and the specificity of the primers and conditions in preliminary studies using Jurkat cell cDNA as a model for monoclonal T cells. Umbilical cord blood mononuclear cells served as a model for polyclonal T cells. Analysis of cDNA obtained from cord blood mononuclear cells and lymphocytes from healthy children showed that our spectratyping conditions are highly accurate and reproducible. The results showed very little skewing of CDR3 length distributions and only a small degree of variation between healthy subjects. The Vβ family CDR3 length distribution commonly conformed to a Gaussian distribution. The distributions of the percentages of relative peaks among the different CDR3 sizes in umbilical cord blood mononuclear cells and T cells from healthy children were remarkably similar.

The methods used to separate T-cell subpopulations were effective in achieving a significant degree of cell purity, allowing us to evaluate CDR3 length diversity within CD45RA and CD45RO cells (26, 27). For example, in analyses of Vβ families within $CD8^+$ CD45RO cells, in which predominant peaks composed over 80% of the area under the curve (Fig. 3 and 4), there was no evidence of contamination within the CD45RA PCR products. Similarly, multiple peaks seen within CD45RA T cells failed to contaminate the predominant cDNA of the $CD8^+$ CD45RO T cells. The considerable degree of resolution of predominant peaks within CD45RA and CD45RO T cells greatly enhanced our analysis of perturbations within the TCR repertoire.

The CDR3 lengths within both the CD45RA and CD45RO T-cell subsets from healthy children and neonates demonstrated a Gaussian distribution. In contrast, we easily detected oligoclonal expansions within $CD8^+$ CD45RO cells that were concealed when unfractionated $CD8^+$ T cells from HIV-infected patients were examined. Patterns of $CD8^+$ T-cell clonal dominance have previously been observed in HIV-infected children on the basis of an evaluation of unfractionated $CD8^+$ T cells (30). Analysis of highly enriched CD45RA and CD45RO $CD8^+$ T cells indicates that clonal predominance may be underestimated if the analysis is limited to unfractionated cells. The $CD8^+$ CD45RO T cells from all four of the HIV-infected children whose cells were examined displayed evidence of oligoclonal expansion. Most importantly, through the enrichment for the CD45 subpopulations and pre-

cise quantitation of CDR3 size diversity, we were able to accurately measure changes that occur within the TCR repertoire during the course of HIV infection.

We easily amplified, cloned, and sequenced CDR3 regions from Jurkat cells and from lymphocytes in cord blood or PBMC. In all cases sequence analysis confirmed the spectratyping findings. All clones from Jurkat cells carried the same amino acid sequences. Polyclonal cord blood or PBMC T cells that had CDR3 lengths which conformed to a Gaussian distribution consisted of cells with a mixture of sequences. Most significantly, a predominant CDR3 peak in $CD8^+$ CD45RO T cells from HIV-infected individuals represented an oligoclonal expansion of a specific TCR clonotype by sequence analysis. These results indicate that spectratyping can be used as an accurate surrogate marker to assess the extent of clonal diversity in healthy and immune-suppressed individuals. We have shown that when TCR CDR3 spectratyping is applied to distinct subpopulations of T cells it can provide a high degree of insight into both the breadth and the specificity of the T-cell immune response. When stringent amplification conditions, precise primers, and effective cell separation techniques are applied together, the diversity of the T-cell immune response can be accurately measured in both health and disease states.

ACKNOWLEDGMENTS

We thank Willam G. Farmerie, Dan Brazeau, and Ginger Clark for help with the GeneScan analysis.

This work was supported by Public Health Service awards RO1 HD32259 and RO1 HL58005, National Institutes of Health-sponsored General Clinical Research Center grant RR0082, an award from the Elizabeth Glazer Pediatric AIDS Foundation (grant PG-50956), and The University of Florida Interdisciplinary Center for Biological Research.

REFERENCES

1. **Akbar, A. N., L. Terry, A. Timms, P. C. Beverley, and G. Janossy.** 1988. Loss of CD45R and gain of UCHL1 reactivity is a feature of primed T cells. J. Immunol. **140:**2171–2178.
2. **Aleixo, L. F., M. M. Goodenow, and J. W. Sleasman.** 1995. Molecular analysis of highly enriched populations of T-cell-depleted monocytes. Clin. Diagn. Lab. Immunol. **2:**733–739.
3. **Brownstein, M. J., J. D. Carpten, and J. R. Smith.** 1996. Modulation of non-templated nucleotide addition by Taq DNA polymerase: primer modifications that facilitate genotyping. BioTechniques **20:**1004–1010.
4. **Callan, M. F., N. Steven, P. Krausa, J. D. Wilson, P. A. Moss, G. M. Gillespie, J. I. Bell, A. B. Rickinson, and A. J. McMichael.** 1996. Large clonal expansions of $CD8^+$ T cells in acute infectious mononucleosis. Nat. Med. **2:** 906–911.
5. **Chen, Z. W., Z. C. Kou, C. Lekutis, L. Shen, D. Zhou, M. Halloran, J. Li, J. Sodroski, D. Lee-Parritz, and N. L. Letvin.** 1995. T cell receptor V beta repertoire in an acute infection of rhesus monkeys with simian immunodeficiency viruses and a chimeric simian-human immunodeficiency virus. J. Exp. Med. **182:**21–31.
6. **Chen, Z. W., Z. C. Kou, L. Shen, J. D. Regan, C. I. Lord, M. Halloran, D. Lee-Parritz, P. N. Fultz, and N. L. Letvin.** 1994. An acutely lethal simian immunodeficiency virus stimulates expansion of V beta 14-expressing T lymphocytes. Proc. Natl. Acad. Sci. USA **91:**7501–7505.
7. **Chen, Z. W., Z. C. Kou, L. Shen, K. A. Reimann, and N. L. Letvin.** 1993. Conserved T-cell receptor repertoire in simian immunodeficiency virus-infected rhesus monkeys. J. Immunol. **151:**2177–2187.
8. **Clement, L. T.** 1992. Isoforms of the CD45 common leukocyte antigen family: markers for human T-cell differentiation. J. Clin. Immunol. **12:**1–10.
9. **Clement, L. T., N. Yamashita, and A. M. Martin.** 1988. The functionally distinct subpopulations of human CD4+ helper/inducer T lymphocytes defined by anti-CD45R antibodies derive sequentially from a differentiation pathway that is regulated by activation-dependent post-thymic differentiation. J. Immunol. **141:**1464–1470.
10. **Connors, M., J. A. Kovacs, S. Krevat, B. J. Gea, M. C. Sneller, M. Flanigan, J. A. Metcalf, R. E. Walker, J. Falloon, M. Baseler, I. Feuerstein, H. Masur, and H. C. Lane.** 1997. HIV infection induces changes in $CD4^+$ T-cell phenotype and depletions within the $CD4^+$ T-cell repertoire that are not immediately restored by antiviral or immune-based therapies. Nat. Med. **3:** 533–540.
11. **De Paoli, P., S. Battistin, and G. F. Santini.** 1988. Age-related changes in human lymphocyte subsets: progressive reduction of the CD4 CD45R (suppressor inducer) population. Clin. Immunol. Immunopathol. **48:**290–296.
12. **Fields, B. A., E. L. Malchiodi, H. Li, X. Ysern, C. V. Stauffacher, P. M. Schlievert, K. Karjalainen, and R. A. Mariuzza.** 1996. Crystal structure of a T-cell receptor beta-chain complexed with a superantigen. Nature **384:**188–192.
13. **Fitzgerald, J. E., N. S. Ricalton, A. C. Meyer, S. G. West, H. Kaplan, C. Behrendt, and B. L. Kotzin.** 1995. Analysis of clonal $CD8^+$ T cell expansions in normal individuals and patients with rheumatoid arthritis. J. Immunol. **154:**3538–3547.
14. **Garcia, K. C., M. Degano, R. L. Stanfield, A. Brunmark, M. R. Jackson, P. A. Peterson, L. Teyton, and I. A. Wilson.** 1996. An alphabeta T cell receptor structure at 2.5 Å and its orientation in the TCR-MHC complex. Science **274:**209–219.
15. **Gea-Banacloche, J. C., E. E. Weiskopf, C. Hallahan, J. C. Lopez Bernaldo de Quiros, M. Flanigan, J. M. Mican, J. Falloon, M. Baseler, R. Stevens, H. C. Lane, and M. Connors.** 1998. Progression of human immunodeficiency virus disease is associated with increasing disruptions within the $CD4^+$ T cell receptor repertoire. J. Infect. Dis. **177:**579–585.
16. **George, J. F., Jr. and H. W. Schroeder, Jr.** 1992. Developmental regulation of D beta reading frame and junctional diversity in T cell receptor-beta transcripts from human thymus. J. Immunol. **148:**1230–1239.
17. **Gorochov, G., A. U. Neumann, A. Kereveur, C. Parizot, T. Li, C. Katlama, M. Karmochkine, G. Raguin, B. Autran, and P. Debre.** 1998. Perturbation of $CD4^+$ and $CD8^+$ T-cell repertoires during progression to AIDS and regulation of the $CD4^+$ repertoire during antiviral therapy. Nat. Med. **4:**215–221.
18. **Grunewald, J., and H. Wigzell.** 1999. T cell receptors in health and disease. Introduction. Springer Semin. Immunopathol. **21:**1–4.
19. **Halapi, E., M. Jeddi-Tehrani, A. Blucher, R. Andersson, P. Rossi, H. Wigzell, and J. Grunewald.** 1999. Diverse T-cell receptor CDR3 length patterns in human $CD4^+$ and $CD8^+$ T lymphocytes from newborns and adults. Scand. J. Immunol. **49:**149–154.
20. **Kostense, S., F. M. Raaphorst, D. W. Notermans, J. Joling, B. Hooibrink, N. G. Pakker, S. A. Danner, J. M. Teale, and F. Miedema.** 1998. Diversity of the T-cell receptor BV repertoire in HIV-1-infected patients reflects the biphasic $CD4^+$ T-cell repopulation kinetics during highly active antiretroviral therapy. AIDS **12:**F235–F240.
21. **Kou, Z. C., M. Halloran, D. Lee-Parritz, L. Shen, M. Simon, P. K. Sehgal, Y. Shen, and Z. W. Chen.** 1998. In vivo effects of a bacterial superantigen on macaque TCR repertoires. J. Immunol. **160:**5170–5180.
22. **Posnett, D. N., R. Sinha, S. Kabak, and C. Russo.** 1994. Clonal populations of T cells in normal elderly humans: the T cell equivalent to "benign monoclonal gammapathy." J. Exp. Med. **179:**609–618. (Erratum, **179:**1077.)
23. **Prochnicka-Chalufour, A., J. L. Casanova, S. Avrameas, J. M. Claverie, and P. Kourilsky.** 1991. Biased amino acid distributions in regions of the T cell receptors and MHC molecules potentially involved in their association. Int. Immunol. **3:**853–864.
24. **Raaphorst, F. M., E. L. Kaijzel, M. J. van Tol, J. M. Vossen, and P. J. van den Elsen.** 1994. Non-random employment of V beta 6 and J beta gene elements and conserved amino acid usage profiles in CDR3 regions of human fetal and adult TCR beta chain rearrangements. Int. Immunol. **6:**1–9.
25. **Schwab, R., P. Szabo, J. S. Manavalan, M. E. Weksler, D. N. Posnett, C. Pannetier, P. Kourilsky, and J. Even.** 1997. Expanded $CD4^+$ and $CD8^+$ T cell clones in elderly humans. J. Immunol. **158:**4493–4499.
26. **Sleasman, J. W., L. F. Aleixo, A. Morton, S. S. Skoda, and M. M. Goodenow.** 1996. $CD4^+$ memory T cells are the predominant population of HIV-1-infected lymphocytes in neonates and children. AIDS **10:**1477–1484.
27. **Sleasman, J. W., T. O. Harville, G. B. White, J. F. George, D. J. Barrett, and M. M. Goodenow.** 1994. Arrested rearrangement of TCR V beta genes in thymocytes from children with X-linked severe combined immunodeficiency disease. J. Immunol. **153:**442–448.
28. **Sleasman, J. W., B. H. Leon, L. F. Aleixo, M. Rojas, and M. M. Goodenow.** 1997. Immunomagnetic selection of purified monocyte and lymphocyte populations from peripheral blood mononuclear cells following cryopreservation. Clin. Diagn. Lab. Immunol. **4:**653–658.
29. **Tedder, T. F., L. T. Clement, and M. D. Cooper.** 1985. Human lymphocyte differentiation antigens HB-10 and HB-11. J. Immunol. **134:**2983–2988.
30. **Than, S., M. Kharbanda, V. Chitnis, S. Bakshi, P. K. Gregersen, and S. Pahwa.** 1999. Clonal dominance patterns of CD8 T cells in relation to disease progression in HIV-infected children. J. Immunol. **162:**3680–3686.
31. **Toyonaga, B., Y. Yoshikai, V. Vadasz, B. Chin, and T. W. Mak.** 1985. Organization and sequences of the diversity, joining, and constant region genes of the human T-cell receptor beta chain. Proc. Natl. Acad. Sci. USA **82:**8624–8628.
32. **Wilson, J. D., G. S. Ogg, R. L. Allen, P. J. Goulder, A. Kelleher, A. K. Sewell, C. A. O'Callaghan, S. L. Rowland-Jones, M. F. Callan, and A. J. McMichael.** 1998. Oligoclonal expansions of CD8(+) T cells in chronic HIV infection are antigen specific. J. Exp. Med. **188:**785–790.